The Poisoning of V_2O_5-WO_3/TiO_2 and V_2O_5-$Ce(SO_4)_2$/TiO_2 SCR Catalysts by KCl and The Partial Regeneration by SO_2

Hua Nie [1,2], Wei Li [1], Qirong Wu [2], Vladislav Rac [3] , Vesna Rakić [3] and Xuesen Du [1,*]

[1] Key Laboratory of Low-Grade Energy Utilization Technologies and Systems, Ministry of Education of People's Republic of China, Chongqing University, Chongqing 400044, China; niehua@spic.com.cn (H.N.); weili19@cqu.edu.cn (W.L.)

[2] State Power Investment Corporation Yuanda Environmental Protection Engineering Co., Ltd., Yancheng 224000, China; wqr20021@126.com

[3] Faculty of Agriculture, University of Belgrade, Nemanjina 6, 11080 Zemun-Belgrade, Serbia; vladarac@agrif.bg.ac.rs (V.R.); vesna.rakic@agrif.bg.ac.rs (V.R.)

* Correspondence: xuesendu@cqu.edu.cn; Tel.: +86-23-6510-3101

Abstract: Poisoning effects by alkali metal chlorides is one of the major reasons for the deactivation of SCR catalyst in biomass-fired plants. In this study, the influence of KCl on two vanadium-based catalysts with different promoters, V_2O_5-WO_3/TiO_2 and V_2O_5-$Ce(SO_4)_2$/TiO_2, was investigated. The catalytic activity of the fresh V_2O_5-WO_3/TiO_2 was higher than that of V_2O_5-$Ce(SO_4)_2$/TiO_2 at low temperatures. V_2O_5-$Ce(SO_4)_2$/TiO_2 performed better than V_2O_5-WO_3/TiO_2 when KCl was deposited on the catalyst surface. Both poisoned catalysts were efficiently regenerated by SO_2 treatment. The characterization results show that the reducibility and acidity of the catalysts were weakened by KCl deposition but regenerated by SO_2.

Keywords: alkali-poisoning; KCl; NH_3-SCR; SO_2 regeneration

1. Introduction

NO_x from exhaust emissions is an important precursor of pollution sources such as smog and acid rain, causing severe damages to the natural environment. Selective catalytic reduction (SCR), with high efficiency of NO_x removal, is a wide-spread technology for reducing the emissions of NO_x from the flue gas of power plants and the exhaust gas of vehicles [1–4]. NO_x is reduced into harmless N_2 by NH_3 over catalysts, following Reactions (1)–(3) with different NO/NO_2 ratios [3,5–7]:

Standard-SCR:

$$4NO + 4NH_3 + O_2 \rightarrow 4N_2 + 6H_2O \tag{1}$$

Fast-SCR:

$$NO + NO_2 + 2NH_3 \rightarrow 2N_2 + 3H_2O \tag{2}$$

NO_2-SCR:

$$6NO_2 + 8NH_3 \rightarrow 7N_2 + 12H_2O \tag{3}$$

Biomass has been used as a renewable fuel due to its environmentally-friendly features. However, the deactivation of the SCR catalyst used in the biomass-fired/cofired boilers is faster than that of coal-fired boilers [8]. The major difference between biomass and fossil fuels is the amount of alkali earth metals contained: it is higher in biofuels than in fossil fuels. Meanwhile, alkali earth metals are always contained in the flue gas and result in the deactivation of SCR [9].

The effect of alkali earth metals on catalysts, especially the commercial VWTi catalysts, has been investigated by many researchers. The activity of SCR catalysts gradually decreases as a result of the alkali accumulation on the catalyst [10]. The acidity of V_2O_5-WO_3/TiO_2 is affected by alkali earth metals owing to the reduction in the concentration of V–OH Brønsted acid sites and the reducibility of active V^{5+} sites, which play a crucial role for the SCR reaction [11–13]. The effect of alkali metals on vanadium active sites has also been confirmed by DFT calculations [11]. V_2O_5-WO_3/TiO_2 is deactivated more seriously by K than Ca and Mg due to the greater decrease in the amount and stability of Brønsted acid sites [14]. The deactivation degree of V_2O_5-WO_3/TiO_2 caused by different forms of calcium follows the order: $CaCO_3 > CaO > CaSO_4$. SO_4^{2-} can partly mitigate the CaO deactivation effect on acid sites [15]. A general method to enhance the alkali-resistance is to deposit promoters on the catalyst surface, which can increase the number of surface acid sites and strengthen their stability, thus improving the alkali metal resistance of commercial SCR catalysts [16]. Cerium, one of the promoters, is proved to enhance V_2O_5/TiO_2 NO_x conversion [17].

Great efforts have been focused on the regeneration of poisoned catalysts and many methods were proposed [18,19], such as water-washing and SO_2-treatment. SO_2 usually appears in the flue gas and leads to SCR catalysts deactivation. NH_4HSO_4 is deposited on the surface through the reaction among SO_2, H_2O, and NH_3, plugging the catalyst pores at low temperatures [20–22]. Ce-based oxide catalytic activity can be significantly enhanced through SO_2-treatment, and the surface acidity of catalyst is strengthened through impregnation with H_2SO_4 solution [22,23]. It is of great interest to study the regeneration of alkali metals-poisoned catalysts through SO_2 treatment.

The impact of KCl on the V_2O_5-WO_3/TiO_2 and V_2O_5-$Ce(SO_4)_2$/TiO_2 catalysts (denoted as VWTi and VCeTi, respectively) was studied. The catalyst poisoning in stationary NO_x sources applications (biomass fired/cofired boilers) was simulated. Experiments were conducted to investigate the regeneration of the poisoned catalysts through SO_2 treatment. The fresh, poisoned, and regenerated catalyst samples were characterized by H_2-TPR and NH_3-TPD experiments. The catalytic activity of the fresh VWTi was higher than that of VCeTi at low temperature, while VCeTi performed better than VWTi when KCl was deposited on the catalyst. SO_2-treatment could efficiently regenerate the poisoned catalysts, especially the VCeTi catalyst.

2. Results and Discussion

2.1. Poisoning Effect of KCl on VWTi Catalyst

Figure 1 illustrates the performance of the VWTi catalyst with different KCl deposition contents under different calcination temperatures. The catalytic activity of VWTi catalysts decreased with increasing of the molar ratio of n(K)/n(V) (i.e., the molar ratio of KCl and V_2O_5), although the calcination temperature (T_{calc}) was different (T_{calc} = 320 and 370 °C; T_{calc} was 20 °C higher than the highest test temperature). Obviously, the catalytic activity decreased significantly owing to the KCl deposition. It indicates that VWTi is susceptible to the alkali species as KCl; especially when the molar ratio of n(K)/n(V) is 1.5, the NO conversion decreased by more than 50%. The results are consistent with the poisoning phenomenon that occur during the operation of a biomass power plant: the catalytic activity decreases due to the deposition and accumulation of KCl. The alkali metal ions (K^+) evaporated from the fuel will absorb on the catalysts surface and form solid KCl particles on the catalyst surface [9]. Moreover, a parallel tendency of the VWTi catalysts calcined at 345, 395, and 420 °C was obtained and N_2-selectivity (>95%) of VWTi catalysts was barely affected by KCl. Figure 2 depicts the NO conversion of poisoned VWTi with different T_{calc}. Fluctuations were clearly observed with different T_{calc}, while all the VWTi catalysts activities dropped due to KCl deposition. The highest point of NO conversion can be explained by the fact that NO conversion of fresh VWTi peaked at 370 °C. The reason for the decrease of NO conversion at 345 °C is that diffusion of small KCl clusters on the catalyst surface led to increasing interface per unit mass of KCl, which is equivalent to the covering of likely active catalytic sites [24–26]. The decreased degree of NO conversion at 345 °C was weakened obviously at

elevated n(K)/n(V). Therefore, the two effects, of alkali metal and the NO conversion fluctuations of fresh catalysts, together led to the results demonstrated in Figure 2.
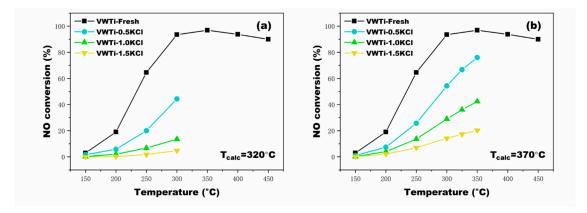

Figure 1. Effects of three n(K)/n(V) ratios on activity of V_2O_5-WO_3/TiO_2 catalyst calcinated at: (**a**) 320 °C; and (**b**) 370 °C.
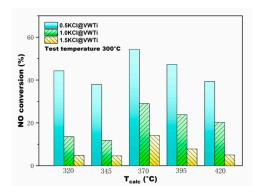

Figure 2. NO conversion of three n(K)/n(V) of KCl poisoned V_2O_5-WO_3/TiO_2 catalysts at different T_{calc}. The test temperature was 300 °C.

2.2. Comparison of Alkali Resistance of VCeTi and VWTi Catalysts

Figure 3 shows the influence of different T_{calc} and molar ratios of n(K)/n(V) on the V_2O_5-$Ce(SO_4)_2$/TiO_2. As illustrated in these figures, the fresh V_2O_5-WO_3/TiO_2 performed better than the fresh V_2O_5-$Ce(SO_4)_2$/TiO_2 at low temperature in terms of activity, whereas their activities were approximately equal at high temperature. Moreover, the NO conversion of all catalysts decreased due to KCl loading. Higher alkali loading imposed a stronger poisoning influence on both VWTi and VCeTi catalysts. One exception is that the VCeTi catalyst was slightly more strongly deactivated when the deposition ratio was 1.0, rather than 1.5, at the calcination temperature of 320 °C. VWTi was sensitive to alkali metal such as potassium, as discussed in Section 2.1, while VCeTi possessed a better alkali resistance than VWTi. It in demonstrated in Figure 3 that the VCeTi exhibited a superior NO conversion than VWTi after poisoning at the test temperature; the explanation for this might be the superior oxidation properties of Ce^{4+} and acidity of SO_4^{2-} [23]. The same experiments were also conducted on poisoned VWTi and VCeTi calcinated at 345, 395 and 420 °C, respectively, and the results are consistent with those discussed above. Figure 4 demonstrates a comparison of poisoned VCeTi calcinated at different temperatures. It can be noticed that the poisoned VCeTi catalytic activity decreased slightly with T_{calc} changing. What is more interesting is that activities of VCeTi catalysts barely changed at n(K)/n(V) = 1.0, 1.5. Based on the experimental results, it can be concluded that VCeTi catalysts possess superior alkaline resistance in a wide calcination temperature window.
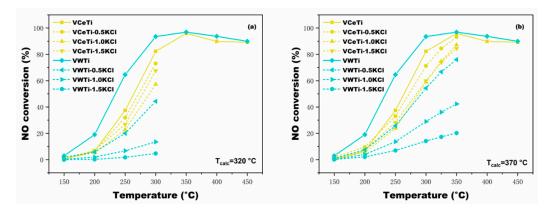
Figure 3. Comparison of activities between V_2O_5-WO_3/TiO_2 and V_2O_5-$Ce(SO_4)_2$/TiO_2 catalyst samples with KCl deposition at different T_{calc}: (**a**) 320 °C; and (**b**) 370 °C.
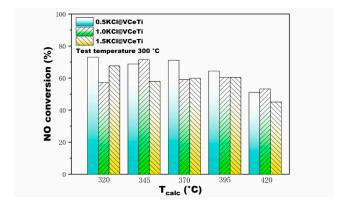

Figure 4. NO conversion of three n(K)/n(V) of KCl poisoned V_2O_5-$Ce(SO_4)_2$/TiO_2 catalyst at different T_{calc}. The test temperature was 300 °C.

2.3. The Regeneration of the Poisoned Catalysts

The regeneration of poisoned catalysts has been investigated by many researchers, and many effective methods have been proposed [27–30]. SO_2 is always contained in the flue gas [27,28]. Consequently, experiments were conducted to explore the regeneration of poisoned catalysts by SO_2 treatment. Figure 5a indicates that the catalytic activity of poisoned VWTi catalysts was dramatically enhanced after SO_2 treatment, even though the activity was still slightly lower than the fresh catalyst. The catalytic activity of regenerated catalysts peaked at T_{calc} = 370 °C, and then decreased at elevated temperature. The regeneration of poisoned VWTi catalysts with 0.5 and 1.0 n(K)/n(V) molar ratios was also investigated. The catalysts with the low molar ratio of n(K)/n(V) possessed a higher NO conversion than the catalysts with the high molar ratio of n(K)/n(V) after regeneration. This observation validates that the deactivation arose from KCl and can be regenerated to some extent.

The SO_2 treatment on poisoned VCeTi catalysts was also employed, and experimental results are plotted in Figure 5b. The activity of poisoned VCeTi was promoted after SO_2 treatment, and barely fluctuated after T_{calc} = 320 °C. It is more interesting that the activity of the regenerated catalyst was even better than that of the fresh catalyst. The reasons for this are more Brønsted acid sites were formed from potassium sulfate and active sites emerged due to surface sulfation by SO_2 [29]. As reported, the number of Brønsted acid sites increased because the surface sulfates on TiO_2 were converted to bidentate surface species (acidic S−OH groups) [30–33], and the reaction rate increased as a result of more Brønsted acid sites [34].
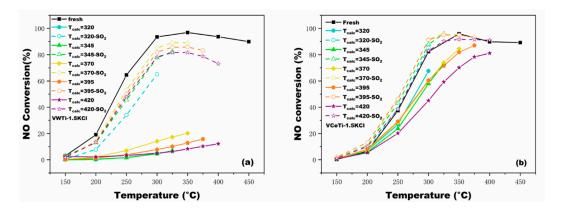
Figure 5. Regeneration effects of: (**a**) poisoned V_2O_5-WO_3/TiO_2 catalyst; and (**b**) poisoned V_2O_5-$Ce(SO_4)_2/TiO_2$ catalyst at n(K)/n(V) = 1.5 through SO_2-treatment. The poisoned catalysts were calcinated at 320, 345, 370, 395, and 420 °C, and the temperature for SO_2-treatment corresponded with calcination temperature.

2.4. Surface Acidity and Redox Properties

NH_3-TPD experiments were employed to investigate the amount and strength of the acid sites on the fresh, poisoned, and regenerated catalysts. The peaks at low (<300 °C) and high (>300 °C) temperature are regarded as weakly chemisorbed NH_3 and strongly chemisorbed NH_3, respectively [35]. Figure 6a shows the curves of NH_3 desorption peak over VWTi catalysts. For poisoned catalyst, the intensity of the NH_3 desorption dramatically decreased at both low and high temperature; especially, the number of strong acids was reduced by 88% according to the integral value of peak area (from 10,374 to 1229) at high temperature. The results are in agreement with those in Reference [36]. Our previous works proposed that 1V5WTi catalyst covers all exposed TiO_2 surface sites [6,37]; both Lewis acid and Brønsted acid sites exist on the VWTi catalyst [38]. Both are also reduced by KCl and result in deactivation, while the number of weak acid sites was extremely enhanced (integral value of the peak area from 3318 to 11,984) through SO_2-treatment, which certified the regeneration by SO_2-treatment. However, the adsorption capacity of a strong acid was nearly the same (integral value of peak area from 1229 to 1255) after regeneration. Based on NH_3-TPD results (Figure 6a) and the NO conversion of fresh, poisoned, and regenerated VWTi catalysts (Figure 5a), it is logical that the NO conversion responsed to the surface acidity variation. Figure 6b demonstrates the NH_3-TPD results of VCeTi catalysts. As for the poisoned VCeTi catalyst, the intensity of the TPD peak dropped slightly, whereas the peak position did not change. After SO_2-treatment, the intensity of weak acid sites improved moderately at low temperatures; however, the intensity of strong acid sites still decreased. This observation suggests that the VCeTi catalytic activity was dominated by Brønsted acid, and the increased Brønsted acid sites strengthened catalytic activity through regeneration [39,40]. The gap of regeneration degree between the poisoned VWTi and VCeTi catalyst can be explained by the fact that the room for surface acidity improved. Since poisoned VCeTi catalyst exhibited a superior surface acidity to poisoned VWTi, the acidity improvement room for poisoned VCeTi was smaller than that of poisoned VWTi (after deposition of KCl, the integral value of NH_3 desorption peak area decreased from 20,245 to 4547 for VWTi, while from 21,862 to 13,912 for VCeTi). Therefore, the regeneration of poisoned VCeTi catalysts by SO_2-treatment is not obvious.

The H_2 consumption of fresh and poisoned catalysts was obtained through H_2-TPR experiments. As shown in Figure 7a, VWTi catalyst exhibited two TPR peaks: TPR Peak (1) at low temperatures shifted towards high temperatures with the deposition of KCl, whereas TPR Peak (2) at high temperatures did not change. Peak (1) was assigned to the reduction of V^{5+} to V^{3+} and W^{6+} to W^{4+} [41], which revealed that the redox ability of V and W was decreased after deposition of KCl, consistent with the activity results. Peak (2) belongs to the reduction of W^{4+} to W^0 [42]. The H_2 consumption peak of fresh VCeTi catalyst contained two overlapped reduction peaks, which can be assigned to V^{5+} and Ce^{4+},

respectively, and a synergistic effect between Ce^{4+} and V^{5+} appeared due to the adjacent peak positions. Through the deposition of KCl, a deviation of the TPR reduction peak was observed, the former peak being related to the reduction of V^{5+} to V^{3+}, while the latter being assigned to the reduction of Ce^{4+} to Ce^{3+} [17,43,44]. It is reported that oxygen vacancies are yielded with the conversion of Ce^{4+} to Ce^{3+} [45]. Oxygen vacancies are beneficial to catalytic activity, thus making VCeTi catalysts perform better than VWTi.
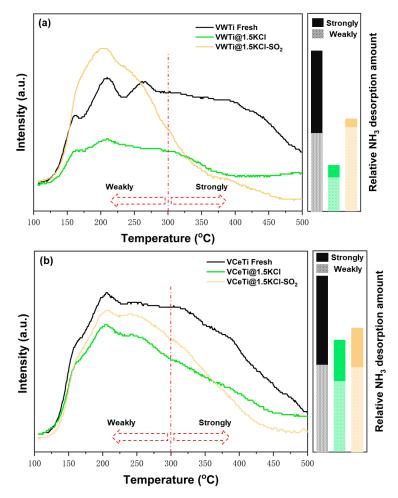

Figure 6. NH$_3$-TPD profiles of the fresh poisoned and regenerated: (**a**) V$_2$O$_5$-WO$_3$/TiO$_2$ catalyst; and (**b**) V$_2$O$_5$-Ce(SO$_4$)$_2$/TiO$_2$ catalyst.
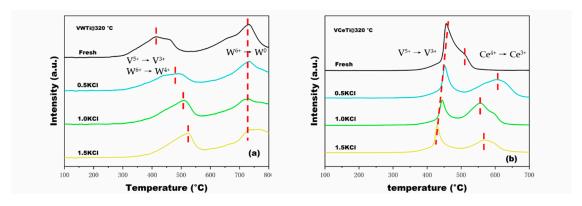
Figure 7. H$_2$-TPR profiles of catalysts at three n(K)/n(V) ratios: (**a**) V$_2$O$_5$-WO$_3$/TiO$_2$; and (**b**) V$_2$O$_5$-Ce(SO$_4$)$_2$/TiO$_2$.

3. Materials and Methods

3.1. Catalyst Synthesis

1 wt.% V_2O_5–5 wt.% WO_3/TiO_2 and 1 wt.% V_2O_5–11.74 wt.% $Ce(SO_4)_2/TiO_2$ (11.74 wt.% $Ce(SO_4)_2$ was calculated according to 5 wt.% CeO_2) were synthesized by the impregnation method. Ammonium vanadate (NH_4VO_3 Aladdin, AP) and ammonium metatungnate (($NH_4)_6H_2W_{12}O_{40}\cdot xH_2O$ Aladdin, AP), used as the precursors of V_2O_5 and WO_3, respectively, were dissolved in deionized water, acidified by oxalic acid, and then vigorously stirred at 60 °C for 30 min. After impregnation of V- and W-precursor on TiO_2 (Degussa, P25, S_{BET} = 55 m^2/g) in a desired proportion, the synthesized samples were dried at 120 °C for 12 h, and subsequently calcinated at 500 °C for 5 h. V_2O_5-$Ce(SO_4)_2/TiO_2$ was prepared by the same method. Ceric sulfate ($Ce(SO_4)_2\cdot4H_2O$ Aladdin AP) was the precursor of $Ce(SO_4)_2$. The detailed synthesis procedure is described in our previous work [46]. The poisoned catalyst was synthesized by impregnation. Potassium chloride (KCl, AP), the alkaline reactant, was dissolved in deionized water and sufficiently stirred, and then mixed with the prepared powdery catalyst according to the molar ratios of n(K)/n(V) = 0.5, 1.0 and 1.5. The catalyst was subsequently dried and then calcinated at 320, 345, 370, 395 and 420 °C to simulate the varying poisoning situations that occur in biomass-fired plants under different operating temperatures.

3.2. Catalytic Performance

The NH_3-SCR reactivity tests were completed on a quartz tube where the catalyst was placed in, and the feed gas of selected composition went through the tube. Meanwhile, the tube was heated by electric furnace. A thermocouple was injected to the bed of the catalyst to monitor the temperature, which was recorded and used in this paper. The feed gas contained 500 ppm NH_3, 500 ppm NO, and 5 vol% O_2 with N_2 as the balance gas. A catalyst sample of 0.5 g with the particle size of 40–60 mesh was used, and the gas hourly space velocity (GHSV) for all experiments was 150,000 $mL\cdot g^{-1}\cdot h^{-1}$. The gas compositions were measured by Protea ProtIR 204M online flue gas analyzer. The value of NO conversion was calculated as follows:

$$\text{NO conversion (\%)} = \frac{[NO]_{in} - [NO]_{out}}{[NO]_{in}} \times 100 \tag{4}$$

3.3. Regeneration Methods

The poisoned catalysts were treated in a quartz tube with a stream of 1000 mL/min mixed gas contained 500 ppm SO_2, 5 vol% O_2 and N_2 as the carrier, under different temperatures (320, 345, 370, 395 and 420 °C, according to the T_{calc}) for 1 h.

3.4. Catalyst Characterization

A PX200A equipment was employed for NH_3 temperature-programmed desorption of ammonia (NH_3-TPD). Powder catalyst (0.2 g) was purged in an atmosphere of 50 mL/min He while the temperature was heated up to 400 °C at 10 °C/min. The purging time was 10 min; then, the sample was cooled gradually down to 100 °C and saturated with 50 mL/min NH_3 and 50 mL/min He for 30 min. After saturation, the sample was purged with pure He at 50 mL/min until the thermal conductivity detector (TCD) signal was stabilized. The signal was collected while the temperature was raised to 500 °C (slope of 10 °C/min).

H_2-temperature programmed reduction (H_2-TPR) was conducted using the PX200A instrument. The catalyst (0.2 g) was purged with pure He at 200 °C for 30 min, and then H_2/Ar mixture gas (10 vol% H_2) was pumped into the reactor with a rate of 50 mL/min. Thirty minutes later, the sample was cooled to ambient temperature in pure He and subsequently heated to 800 °C at a rate of 10 °C/min under 10 vol% H_2/Ar. The values of H_2 consumption were obtained through TCD.

4. Conclusions

This systematic experimental investigation focused on the effects of KCl and SO_2 on V_2O_5-WO_3/TiO_2 and V_2O_5-$Ce(SO_4)_2$/TiO_2. V_2O_5-WO_3/TiO_2 and V_2O_5-$Ce(SO_4)_2$/TiO_2 were calcinated at different temperatures. Their catalytic activities were inhibited by KCl loading with different molar ratios. The characterization afterwards showed that the reducibility and acidity of V_2O_5-WO_3/TiO_2 and V_2O_5-$Ce(SO_4)_2$/TiO_2 were remarkably decreased by KCl. V_2O_5-$Ce(SO_4)_2$/TiO_2 exhibited a superior alkali metal resistance to V_2O_5-WO_3/TiO_2; the poisoned catalytic activity can be efficiently regenerated through SO_2 treatment. V_2O_5-$Ce(SO_4)_2$/TiO_2 even possessed a better activity than the fresh catalyst.

Author Contributions: Conceptualization, H.N.; Formal analysis, V.R. (Vladislav Rac) and V.R. (Vesna Rakić); Funding acquisition, X.D.; Investigation, H.N. and Q.W.; Resources, X.D.; Supervision, X.D.; Writing – original draft, W.L.; Writing – review & editing, X.D. All authors have read and agreed to the published version of the manuscript.

Conflicts of Interest: The authors declare no conflict of interest.

References

1. Taylor, K.C. Nitric oxide catalysis in automotive exhaust systems. *Catal. Rev. Sci. Eng.* **1993**, *35*, 457–481. [CrossRef]
2. Busca, G.; Lietti, L.; Ramis, G.; Berti, F. Chemical and mechanistic aspects of the selective catalytic reduction of NO_x by ammonia over oxide catalysts: A review. *Appl. Catal. B Environ.* **1998**, *18*, 1–36. [CrossRef]
3. Lai, J.-K.; Wachs, I.E. A Perspective on the Selective Catalytic Reduction (SCR) of NO with NH_3 by Supported V_2O_5–WO_3/TiO_2 Catalysts. *ACS Catal.* **2018**, *8*, 6537–6551. [CrossRef]
4. Wang, X.; Du, X.; Xue, J.; Yang, G.; Chen, Y.; Zhang, L. New insights into the N_2O formation mechanism during selective catalytic reduction of NO_x with NH_3 over V-based catalyst. *Catal. Today* **2019**. [CrossRef]
5. Grossale, A.; Nova, I.; Tronconi, E.; Chatterjee, D.; Weibel, M. NH_3-NO/NO_2 SCR for Diesel Exhausts Aftertreatment: Reactivity, Mechanism and Kinetic Modelling of Commercial Fe- and Cu-Promoted Zeolite Catalysts. *Top. Catal.* **2009**, *52*, 1837–1841. [CrossRef]
6. Wang, X.; Du, X.; Zhang, L.; Chen, Y.; Yang, G.; Ran, J. Promotion of NH_4HSO_4 decomposition in NO/NO_2 contained atmosphere at low temperature over V_2O_5-WO_3/TiO_2 catalyst for NO reduction. *Appl. Catal. A Gen.* **2018**, *559*, 112–121. [CrossRef]
7. Wang, X.; Du, X.; Liu, S.; Yang, G.; Chen, Y.; Zhang, L.; Tu, X. Understanding the deposition and reaction mechanism of ammonium bisulfate on a vanadia SCR catalyst: A combined DFT and experimental study. *Appl. Catal. B Environ.* **2020**, *260*, 118168. [CrossRef]
8. Khodayari, R.; Andersson, C.; Odenbrand, I.; Andersson, L.A. Deactivation and regeneration of SCR catalysts used in bio fuel power plants. In Proceedings of the 5th European Conference on Industrial Furnaces and Boilers, Porto, Portugal, 11–14 April 2000; pp. 543–554.
9. Zheng, Y.; Jensen, A.D.; Johnsson, J.E. Laboratory Investigation of Selective Catalytic Reduction Catalysts: Deactivation by Potassium Compounds and Catalyst Regeneration. *Ind. Eng. Chem. Res.* **2004**, *43*, 941–947. [CrossRef]
10. Kling, Å.; Andersson, C.; Myringer, Å.; Eskilsson, D.; Järås, S.G. Alkali deactivation of high-dust SCR catalysts used for NO_x reduction exposed to flue gas from 100MW-scale biofuel and peat fired boilers: Influence of flue gas composition. *Appl. Catal. B Environ.* **2007**, *69*, 240–251. [CrossRef]

11. Nicosia, D.; Czekaj, I.; Kröcher, O. Chemical deactivation of V$_2$O$_5$/WO$_3$–TiO$_2$ SCR catalysts by additives and impurities from fuels, lubrication oils and urea solution: Part II. Characterization study of the effect of alkali and alkaline earth metals. *Appl. Catal. B Environ.* **2008**, *77*, 228–236. [CrossRef]

12. Peng, Y.; Li, J.; Si, W.; Luo, J.; Wang, Y.; Fu, J.; Li, X.; Crittenden, J.; Hao, J. Deactivation and regeneration of a commercial SCR catalyst: Comparison with alkali metals and arsenic. *Appl. Catal. B Environ.* **2015**, *168-169*, 195–202. [CrossRef]

13. Janssen, F.J.; Van den Kerkhof, F.M.; Bosch, H.; Ross, J.R. Mechanism of the reaction of nitric oxide, ammonia, and oxygen over vanadia catalysts. I. The role of oxygen studied by way of isotopic transients under dilute conditions. *J. Phys. Chem.* **1987**, *91*, 5921–5927. [CrossRef]

14. Chen, L.; Li, J.; Ge, M. The poisoning effect of alkali metals doping over nano V$_2$O$_5$–WO$_3$/TiO$_2$ catalysts on selective catalytic reduction of NO$_x$ by NH$_3$. *Chem. Eng. J.* **2011**, *170*, 531–537. [CrossRef]

15. Li, X.; Li, X.; Yang, R.T.; Mo, J.; Li, J.; Hao, J. The poisoning effects of calcium on V2O5-WO3/TiO2 catalyst for the SCR reaction: Comparison of different forms of calcium. *Mol. Catal.* **2017**, *434*, 16–24. [CrossRef]

16. Li, H.; Miao, J.; Su, Q.; Yu, Y.; Chen, Y.; Chen, J.; Wang, J. Improvement in alkali metal resistance of commercial V$_2$O$_5$–WO$_3$/TiO$_2$ SCR catalysts modified by Ce and Cu. *J. Mater. Sci.* **2019**, *54*, 14707–14719. [CrossRef]

17. Liu, Z.; Zhang, S.; Li, J.; Zhu, J.; Ma, L. Novel V$_2$O$_5$–CeO$_2$/TiO$_2$ catalyst with low vanadium loading for the selective catalytic reduction of NOx by NH3. *Appl. Catal. B Environ.* **2014**, *158–159*, 11–19. [CrossRef]

18. Jin, R.; Liu, Y.; Wu, Z.; Wang, H.; Gu, T. Relationship between SO$_2$ poisoning effects and reaction temperature for selective catalytic reduction of NO over Mn–Ce/TiO$_2$ catalyst. *Catal. Today* **2010**, *153*, 84–89. [CrossRef]

19. Chang, H.; Li, J.; Yuan, J.; Chen, L.; Dai, Y.; Arandiyan, H.; Xu, J.; Hao, J. Ge, Mn-doped CeO$_2$–WO$_3$ catalysts for NH$_3$–SCR of NOx: Effects of SO$_2$ and H$_2$ regeneration. *Catal. Today* **2013**, *201*, 139–144. [CrossRef]

20. Guo, X.; Bartholomew, C.; Hecker, W.; Baxter, L.L. Effects of sulfate species on V$_2$O$_5$-WO$_3$/TiO$_2$ SCR catalysts in coal and biomass-fired systems. *Appl. Catal. B Environ.* **2009**, *92*, 30–40. [CrossRef]

21. Magnusson, M.; Fridell, E.; Ingelsten, H.H. The influence of sulfur dioxide and water on the performance of a marine SCR catalyst. *Appl. Catal. B Environ.* **2012**, *111–112*, 20–26. [CrossRef]

22. Ye, D.; Qu, R.; Zheng, C.; Cen, K.; Gao, X. Mechanistic investigation of enhanced reactivity of NH$_4$HSO$_4$ and NO on Nb- and Sb-doped VW/Ti SCR catalysts. *Appl. Catal. A Gen.* **2018**, *549*, 310–319. [CrossRef]

23. Hu, W.; Zhang, Y.; Liu, S.; Zheng, C.; Gao, X.; Nova, I.; Tronconi, E. Improvement in activity and alkali resistance of a novel V-Ce(SO4)2/Ti catalyst for selective catalytic reduction of NO with NH3. *Appl. Catal. B Environ.* **2017**, *206*, 449–460. [CrossRef]

24. López Granados, M.; Galisteo, F.C.; Lambrou, P.S.; Mariscal, R.; Sanz, J.; Sobrados, I.; Fierro, J.L.G.; Efstathiou, A.M. Role of P-containing species in phosphated CeO$_2$ in the deterioration of its oxygen storage and release properties. *J. Catal.* **2006**, *239*, 410–421. [CrossRef]

25. Larese, C.; López Granados, M.; Mariscal, R.; Fierro, J.L.G.; Lambrou, P.S.; Efstathiou, A.M. The effect of calcination temperature on the oxygen storage and release properties of CeO$_2$ and Ce–Zr–O metal oxides modified by phosphorus incorporation. *Appl. Catal. B Environ.* **2005**, *59*, 13–25. [CrossRef]

26. Larese, C.; Galisteo, F.C.; Granados, M.L.; Mariscal, R.; Fierro, J.L.G.; Lambrou, P.S.; Efstathiou, A.M. Effects of the CePO$_4$ on the oxygen storage and release properties of CeO$_2$ and Ce$_{0.8}$Zr$_{0.2}$O$_2$ solid solution. *J. Catal.* **2004**, *226*, 443–456. [CrossRef]

27. Jecht, U. Flue Gas Analysis in Industry. Practical guide for Emission and Process Measurements. *Testo* **2004**, 1–145.

28. Zevenhoven, R.; Kilpinen, P. *Control of Pollutants in Flue Gases and Fuel Gases*; Helsinki University of Technology Espoo: Espoo, Finland, 2001.

29. Yang, S.; Guo, Y.; Chang, H.; Ma, L.; Peng, Y.; Qu, Z.; Yan, N.; Wang, C.; Li, J. Novel effect of SO$_2$ on the SCR reaction over CeO$_2$: Mechanism and significance. *Appl. Catal. B Environ.* **2013**, *136*, 19–28. [CrossRef]

30. Waqif, M.; Bachelier, J.; Saur, O.; Lavalley, J.-C. Acidic properties and stability of sulfate-promoted metal oxides. *J. Mol. Catal.* **1992**, *72*, 127–138. [CrossRef]

31. Saur, O.; Bensitel, M.; Saad, A.M.; Lavalley, J.; Tripp, C.P.; Morrow, B. The structure and stability of sulfated alumina and titania. *J. Catal.* **1986**, *99*, 104–110. [CrossRef]

32. Busca, G.; Saussey, H.; Saur, O.; Lavalley, J.C.; Lorenzelli, V. FT-IR characterization of the surface acidity of different titanium dioxide anatase preparations. *Appl. Catal.* **1985**, *14*, 245–260. [CrossRef]

33. Yuan, H.; He, J.; Li, R.; Ma, X. Characterization of SO$_4^{2-}$/TiO$_2$ and its catalytic activity in the epoxidation reaction. *Res. Chem. Intermed.* **2017**, *43*, 4353–4368. [CrossRef]

34. Amiridis, M.D.; Wachs, I.E.; Deo, G.; Jehng, J.-M. Reactivity of V_2O_5 catalysts for the selective catalytic reduction of NO by NH_3: Influence of vanadia loading, H_2O, and SO_2. *J. Catal.* **1996**, *161*, 247–253. [CrossRef]

35. Jo, D.; Park, G.T.; Ryu, T.; Hong, S.B. Economical synthesis of high-silica LTA zeolites: A step forward in developing a new commercial NH3-SCR catalyst. *Appl. Catal. B Environ.* **2019**, *243*, 212–219. [CrossRef]

36. Wang, X.; Cong, Q.; Chen, L.; Shi, Y.; Shi, Y.; Li, S.; Li, W. The alkali resistance of CuNbTi catalyst for selective reduction of NO by NH3: A comparative investigation with VWTi catalyst. *Appl. Catal. B Environ.* **2019**, *246*, 166–179. [CrossRef]

37. Wang, X.; Du, X.; Zhang, L.; Yang, G.; Chen, Y.; Ran, J. Simultaneous Fast Decomposition of NH_4HSO_4 and Efficient NO_x Removal by NO_2 Addition: An Option for NO_x Removal in H_2O/SO_2-Contained Flue Gas at a Low Temperature. *Energy Fuels* **2018**, *32*, 6990–6994. [CrossRef]

38. Zhu, M.; Lai, J.-K.; Tumuluri, U.; Wu, Z.; Wachs, I.E. Nature of active sites and surface intermediates during SCR of NO with NH_3 by supported V_2O_5-WO_3/TiO_2 catalysts. *J. Am. Chem. Soc.* **2017**, *139*, 15624–15627. [CrossRef]

39. Zhang, T.; Qu, R.; Su, W.; Li, J. A novel Ce–Ta mixed oxide catalyst for the selective catalytic reduction of NO_x with NH_3. *Appl. Catal. B Environ.* **2015**, *176*, 338–346. [CrossRef]

40. Chen, L.; Li, J.; Ge, M. DRIFT Study on Cerium− Tungsten/Titiania Catalyst for Selective Catalytic Reduction of NO_x with NH_3. *Environ. Sci. Technol.* **2010**, *44*, 9590–9596. [CrossRef]

41. Li, X.; Li, X.; Chen, J.; Li, J.; Hao, J. An efficient novel regeneration method for Ca-poisoning V_2O_5-WO_3/TiO_2 catalyst. *Catal. Commun.* **2016**, *87*, 45–48. [CrossRef]

42. Kompio, P.G.W.A.; Brückner, A.; Hipler, F.; Auer, G.; Löffler, E.; Grünert, W. A new view on the relations between tungsten and vanadium in $V_2O_5WO_3$/TiO_2 catalysts for the selective reduction of NO with NH_3. *J. Catal.* **2012**, *286*, 237–247. [CrossRef]

43. Peng, Y.; Wang, C.; Li, J. Structure–activity relationship of VO_x/CeO_2 nanorod for NO removal with ammonia. *Appl. Catal. B Environ.* **2014**, *144*, 538–546. [CrossRef]

44. Ma, Z.; Wu, X.; Si, Z.; Weng, D.; Ma, J.; Xu, T. Impacts of niobia loading on active sites and surface acidity in NbO_x/CeO_2–ZrO_2 NH_3–SCR catalysts. *Appl. Catal. B Environ.* **2015**, *179*, 380–394. [CrossRef]

45. Ke, Y.; Huang, W.; Li, S.; Liao, Y.; Li, J.; Qu, Z.; Yan, N. Surface acidity enhancement of CeO_2 catalysts via modification with a heteropoly acid for the selective catalytic reduction of NO with ammonia. *Catal. Sci. Technol.* **2019**, *9*, 5774–5785. [CrossRef]

46. Chen, Y.; Wang, M.; Du, X.; Ran, J.; Zhang, L.; Tang, D. High Resistance to Na Poisoning of the V_2O_5-Ce$(SO_4)_2$/TiO_2 Catalyst for the NO SCR Reaction. *Aerosol Air Qual. Res.* **2018**, *18*, 2948–2955. [CrossRef]